View metadata, citation and similar papers at core.ac.uk

brought to you by CORE

provided by CERN Document Server

Available on CMS information server

CMS NOTE 2006/141

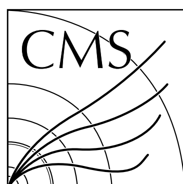

The Compact Muon Solenoid Experiment

CMS Note

Mailing address: CMS CERN, CH-1211 GENEVA 23, Switzerland

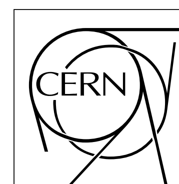

11 October 2006

The Qualification of Silicon Microstrip Detector Modules for the CMS Inner Tracking Detector

M. Axer[b)], F. Beißel, G. Flügge, T. Franke, Th. Hermanns[a)], J. Mnich[c)], A. Nowack, M. Pöttgens, O. Pooth

III. Physikalisches Institut B, RWTH Aachen University

On behalf of the CMS Silicon Tracker Collaboration

Abstract

For the construction of the CMS inner tracking detector 15,232 silicon microstrip detectors had to be produced. This large number required a fast, easy to use and cost-efficient test setup for the quality assurance at different production steps in all laboratories participating in the production of the detector modules. This article describes typical faults occurring on modules as well as the test procedures used to identify and classify them provided by the APV Readout Controller (ARC) system. To establish the final test procedures the data of more than 500 tracker endcap modules had been analysed in detail. An optimal combination of measures was found that prove to be extremely efficient in detecting and properly identifying all relevant failure modes of a detector module. Finally the quality of all modules for the CMS silicon microstrip tracker is quoted.

a) Thomas.Hermanns@cern.ch

b) now at Institut für Medizin, Forschungszentrum Jülich

c) now at DESY, Hamburg

1 Introduction

The inner tracking system of the future Large Hadron Collider [1] experiment Compact Muon Solenoid (CMS) [2] consists of the inner vertex detector which is based on silicon pixel sensors and the outer tracking detector which is constructed of silicon microstrip detectors [3, 4]. The main components of the latter are one or two silicon sensors which provide the sensitive area for detecting particles, and the frontend hybrid [5] which is a printed circuit board mounted close to the silicon that supports the electronics necessary for readout (mainly via 4 or 6 APV-chips [6]) and control of the detector modules. It is connected to the sensors via an interface, the pitch-adapter, by means of wire-bonds.[1)]

A silicon detector module is the smallest independent unit for particle detection of the CMS microstrip tracker and in total 15,232 of them had to be assembled and qualified. The individual subcomponents were produced in industry, whereas assembly and electrical connections were done by the collaborating institutes. Due to the large scale of the CMS tracker various laboratories/institutes had to be involved and therefore components and partially finished modules had to be transferred regularly among the sites.

The quality constraints on module production and assembly were very demanding. Thorough tests at each step of production had to be performed to avoid the usage of defective components in order to insert only the best functioning modules into the tracker. Besides standard methods of quality control like visual inspections the APV Readout Controller (ARC) system was designed as a dedicated test system. Though it was originally intended to be used only for verifying the quality of hybrids [7], the test system was later upgraded to include sensor tests. A high voltage supply and LED system fulfil the hardware requirements to qualify a complete module by detecting single channel faults. In parallel with the development of the hardware, a special readout- and test-software (APV Readout Controller Software) was written. A detailed description of the implementation of the LabView based Graphical User Interface and the more sophisticated C++ hardware access and data analysis routines is presented in [8].

By means of the completely automated test procedure and analysis of the ARC system the failures on modules can be readily identified. Details about possible faults and the strategies to uncover them are described in chapter 2. In section 3 the suitability of certain tests in identifying the typical faults is studied while the efficiency of the results of this investigation is discussed in chapter 4. Finally conclusive results about the efficiency of the qualification and the quality of the modules themselves are presented in chapter 5.

2 The Signatures of Faults in Different Tests

There are a variety of possible faults that can occur in silicon strip modules such as those used by CMS. These are related to defects of the p-n-diode structure of the silicon sensor itself (Fig. 1) or to the readout of a module via the hybrid. Details of the sensor are given in [9].

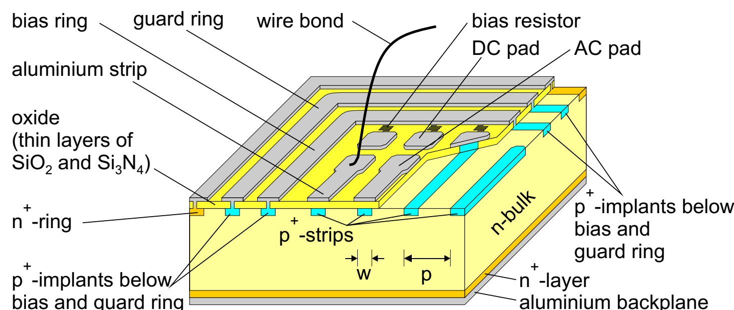

Figure 1: The CMS silicon microstrip detector module design according to [9].

2.1 The Test Environment

All tests are performed at room temperature in a metal box which serves for the protection of the module during the test, shields the module from environmental noise, ensures darkness to minimise the leakage current of the silicon sensors, and makes a sufficiently gas-tight volume to allow dry air flushing to suppress surface currents while the

[1)] Frontend hybrid and detector module are denoted in the following sections only as hybrid and module, respectively.

sensors are biased. By the design of the box a module can be mounted quickly as connections to the ARC system, the high voltage supply, and the LED system are arranged permanently inside the box volume so that only two simple connections to the modules are required before tests can start.

2.2 The Problems and Flaws Affecting the Performance of a Module

The most frequent failure on a module is an *open bond*. In that case a channel is disconnected from the readout electronics because of a missing or broken electrical wire-bond connection at the APV-preamplifier input or on the pitch adapter (pitch adapter-sensor-open). In modules having two sensors connected serially, this failure can also occur between the sensors (sensor-sensor-open). Similarly a break in the metallization of a strip on a sensor will be referred to as a broken strip and is also assigned to this category of fault.

If at least two neighbouring strips are connected electrically by sensor production imperfections these microstrips are considered to be *short-circuited channels*. Other short-circuited conductor paths, e. g. bond wires that touch each other, also belong to this type of failure.

The failure that is denoted as a *pinhole* reveals a short-circuited or ohmic contact between an aluminium microstrip and its underlying p^+-implant that is normally ac coupled [10]. *Dead channels* are the result of a defective APV-preamplifier input of the dedicated readout channel.

If there is a significant difference in operating the APV-chip with activated or deactivated signal inversion one classifies the affected channels as having a *defective inverter*. Another failure assesses the APV-internal matrix for buffering signals (pipeline), which might have *noisy or dead pipeline storage cells*.

The last category of recognized failures includes failures, which affect not only single channels but a whole chip on the hybrid or even an entire hybrid or module. During a *high voltage breakdown* the bias current of the module exceeds certain limits before reaching the operational voltage while in the case of *problems with the hybrid operation* one observes errors like an irregular power consumption of the hybrid, failures in I^2C-communication with a chip on the hybrid, or asynchronous behaviour of the APV readout chips.

2.3 The Pre-Qualifying Tests

Deep and time-consuming tests are reasonable only if the quality of the sensors is acceptable and the readout electronics is operating properly. For that reason a current-voltage scan (IV-test) and the Functional Test pre-qualify a module. The number of modules not passing these two tests is negligible because suspicious components, which might cause the failure of tests, are not assembled to modules.

2.3.1 IV-Test

During the IV-test, the bias voltage of the silicon sensor is ramped up to 450 V while the bias current is recorded. A typical value for the maximum current of a “good” module is $\mathcal{O}$(0.1 to 1 μA), depending on the size of the sensor. If the total current at 450 V exceeds 3 μA (module with one sensor) or 6 μA (module with two sensors) the module is marked as “suspicious”. Currents higher than 10 or 20 μA qualify a module as “bad” and the execution of further tests is aborted. At the end of a passed IV-test a fixed voltage of 400 V is established so that all subsequent tests are performed with the silicon sensor overdepleted.

2.3.2 Functional Test

The Functional Test procedure includes nine basic functionality tests intended for a fast characterization of the hybrids. At first the proper functioning of the test system itself is verified while the following tests incorporate the validation of the I^2C communication, basic chip functionalities, and power consumption. In case of a serious problem or failure on the hybrid the whole test sequence is stopped.

2.4 Pedestal and Noise Test

The pedestal for each channel is defined as the average strip output level without any particle (or calibration) signal. As the pedestal data are not very sensitive to typical hybrid or module failures, they are mainly used for data correction and noise calculation purposes.

The RMS fluctuation of the raw data of a channel around its pedestal is called *raw noise*. Due to electronic noise pick-up at the inputs of the APV-preamplifier an event by event baseline shift common to groups of neighbouring or all channels of a module occurs. This effect is called *common mode noise*. Correcting the raw noise for these shifts, one derives the *common mode subtracted noise* for each channel. This quantity assesses the quality of a channel with respect to its noise behaviour (Fig. 2).

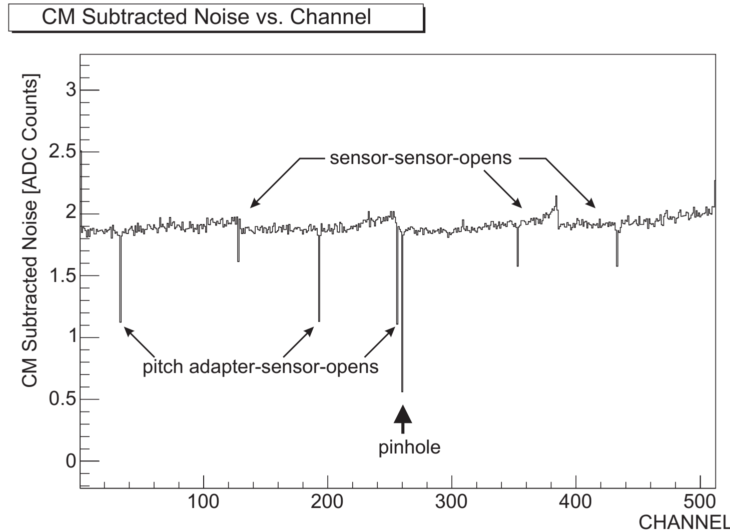

Figure 2: Behaviour of open bonds and pinholes in the common mode subtracted noise.

Depending on the type of a fault, specific deviations from the noise of normal, i. e. faultless, channels can be observed. As the noise increases with an increasing capacitance, which, in turn, is determined by the length of the strip connected to the input of the APV-preamplifier, open bonds between the two sensors (sensor-sensor-opens) result in a lower noise, whereas pitch adapter-sensor-opens result in even lower noise. Pinholes and dead channels show the least noise because they do not respond to any signal. The noise of short-circuited channels does not behave uniquely but it has an abnormal value in at least one of the four possible APV operation modes.

2.5 Common Mode Noise Measurement

The mentioned consideration concerning the noise level of different types of faults applies only if the common mode shifts are minimised. Normal channels pick up these fluctuations as a common mode noise, whereas channels with open bonds do not or only partially participate in these shifts. After common mode subtraction, channels with open bonds can imitate a higher signal and hence more noise. Therefore the dependency of the common mode subtracted noise on the common mode noise is more pronounced for a missing bond at the pitch adapter compared to an open between sensors.

2.6 Calibration Pulse Shape Test

The Calibration Pulse Shape Test uses an APV-internal calibration signal circuit. It measures the amplitude, the peak time, and the rise time of a charge signal, which is adjusted to an equivalent of two minimum ionising particles (about 50,000 e^- for a sensor of 320 μm thickness). The total charge signal is injected successively into eight APV-calibration groups consisting of 16 channels each.

The peak time of a signal in a channel with a lower capacitance connected to the input of the APV-preamplifier decreases because of a lower time constant and hence a faster rise time of the signal. The deviation of these open bond-channels from the average of normal ones as well as the distinction of their different locations stands out clearly in the data (Fig. 3).

Besides the detection of open bonds and pinholes, the pulse height test is mainly used to indicate short-circuited strips (Fig. 4). The charge injected into one of these strips spreads over all of them such that the amplitude of the signal read out from one of the strips decreases. Finally the absolute ratio of the signal amplitude per channel with activated and deactivated APV-inverter reveals problems with the inverter electronics if it differs more than 25% from unity.

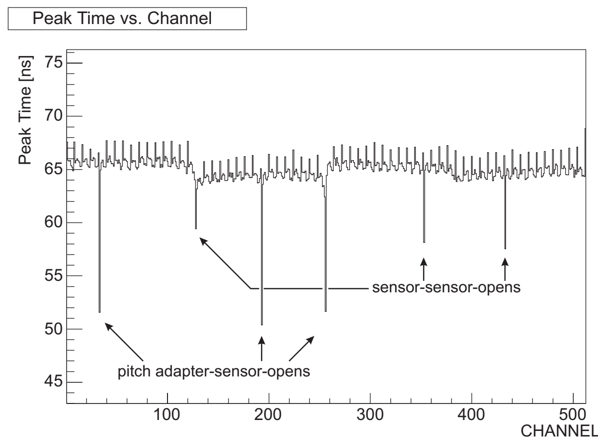

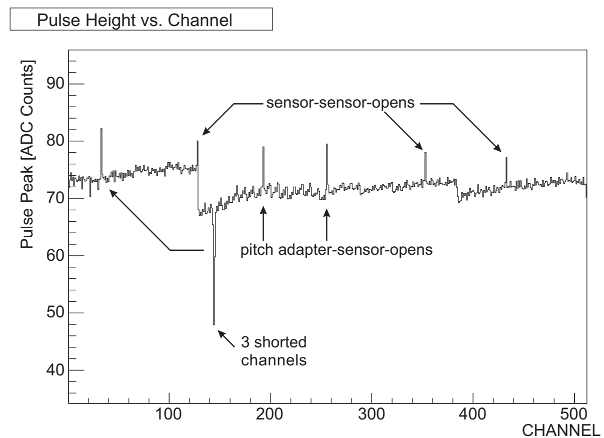

Figure 3: Behaviour of the different types of open bonds for the peak time measurement. The spiny structure above the majority of cases stems from the calibration logic that supplies the signal to every eighth channel at the same time.

Figure 4: Behaviour of defective channels, especially shorts, for the pulse height measurement.

2.7 Pipeline Test

To detect noisy and dead pipeline cells, the pedestal, the noise and the amplitude of a calibration signal for each cell of the APV-internal storage matrix are determined. For each channel these quantities should be independent from a specific cell, so that a deviation of more than a factor of two with respect to the median value of a channel indicates a defective cell.

2.8 Gain Test

The Gain Test measures the amplitude of a calibration signal as a function of the injected charge for each channel. As long as the charge corresponds to less than three minimum ionising particles the data are well described by a linear fit function, of which the slope, the offset and the χ^2 are evaluated. A large χ^2 value of the fit indicates a non-linearity. Due to the simplicity of the fit the results are very robust and suited to finding all types of faults that influence the amplitude of the charge signal, i.e. open bonds, short-circuited channels, dead channels, and pinholes.

2.9 Backplane Pulse Test

During the Backplane Pulse Test an offset of about 2 V is added to the bias voltage within a period of about 10 ns. While for normal channels this signal is equalised almost completely by an APV-internal common mode correction, a large signal is induced for channels that only participate partially in the common mode shifts. Therefore this test can both identify and precisely localize open bonds.

2.10 Pinhole Test

In order to detect pinholes the ARC-software measures the amplitude of calibration signals as a function of the photo-current of the sensor. The latter is adjusted continously using infrared LED-light to a maximum of 300-500 μA. Only the response to signals of strips with pinholes varies as a function of the LED intensity [10], in particular if the electrical breakthrough between p^+-implant and aluminium microstrip occurs only at high currents and for a large potential difference between them. The channelwise maximum calibration pulse amplitude difference calculated from the results of the light intensity scan reveals pinholes very clearly (Fig. 5). Finally only this test can reliably differentiate between pinholes and dead channels, which do not follow the rising and falling of the signal when varying the photo-current.

3 The Optimisation of the Fault Finding Algorithm

As discussed in section 2, there are numerous criteria to identify and to classify different types of faults. Nevertheless the significance of deviations from the behaviour of normal channels depends on the specific module

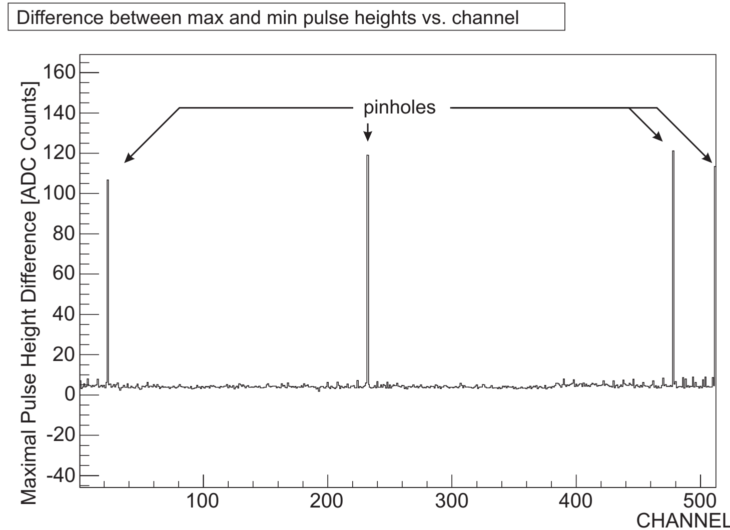

Figure 5: Detection of pinholes by the difference between the maximum and minimum measured pulse height per channel.

geometry, the APV operation mode, the test setup, and the relative importance of superimposed structures in the data that might be of the same order (see for example Fig. 4).

Thus a fault finding algorithm, which should be based on redundant information from different tests, should provide an appropriate robustness in flagging defects. This can be achieved only if the most significant test results are considered to reduce the rate of falsely flagged good channels and to facilitate the classification of the type of fault.

The data for about 500 modules of all geometries of the CMS silicon tracker endcaps acquired at seven different laboratories were collected. As many of these modules were tested more than once, a data set of about 1000 complete tests with the ARC system (corresponding to about 675,000 readout channels) was investigated [11]. For each measurement the following quantities were inspected individually:

- Pedestal
- Common Mode Subtracted Noise
- Calibration Pulse Amplitude
- Calibration Pulse Peak Time
- Calibration Pulse Rise Time
- Gain Slope
- Pinhole Test Maximum Calibration Pulse Amplitude
- Pinhole Test Maximum Calibration Pulse Amplitude Difference

Based on these quantities, 743 open bonds (localised exactly by means of a microscope), 128 short-circuited channels, 114 dead channels and 109 pinholes could be identified for the entire dataset.

3.1 Processing of Measured Data

As some measures depend strongly on the characteristics of individual APV-chips, as well as the sensor geometry, the deviation of faults has to be referred to APV-mean values and considered separately for each sensor geometry. For this reason the following methods of processing for the above listed measures were accumulated in histograms:

- absolute values (*ABS*),
- relative values with respect to the median value which is less sensitive to large single channel fluctuations than the mean value (*PERC*),

- absolute deviations from the median value (*ABSDEV_0*),
- relative values with respect to the prediction of a polynomial fit (of first to third degree) (*PERC_1* to *PERC_3*),
- absolute deviations from the prediction of a polynomial fit (of first to third degree) (*ABSDEV_1* to *ABSDEV_3*),
- absolute deviations from the median of the dedicated calibration injection group (*CALGR*) (only for tests where the APV calibration circuit is used).

The superposition of histograms of different faults reveals the separation not only from normal but also of various types of faulty channels. As the quality of the separation depends significantly on the type of data processing (Fig. 6 and Fig. 7), the suitability of a certain test and a certain processing is assessed by means of two criteria derived from these histograms, as explained in the following subsections.

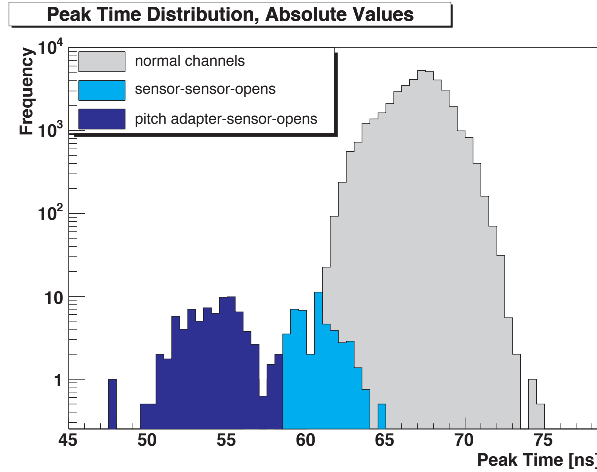

Figure 6: The separation of channels with open bonds in the *ABS*-processed peak time.

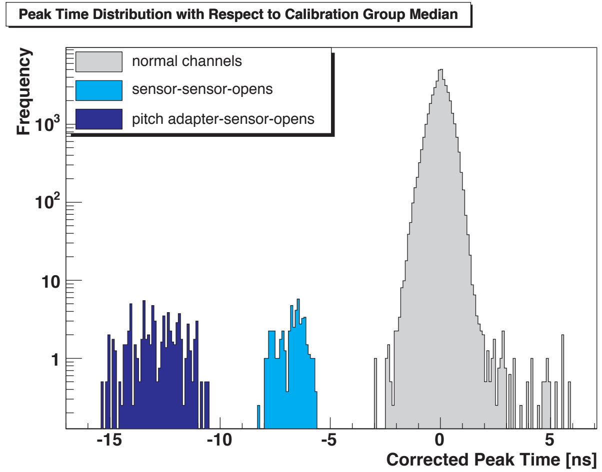

Figure 7: The separation of channels with open bonds in the *CALGR*-processed peak time.

3.1.1 The Distance Criterion

By calculating the mean value and the RMS for each histogram the distance D can be derived, to separate normal channels (type 1) from, for instance, channels with open bonds (type 2) etc.

$$D = \frac{|\text{mean}_1 - \text{mean}_2|}{\text{RMS}_1 + \text{RMS}_2}. \tag{1}$$

The larger the difference between the mean values and the smaller the RMS of the distributions is, the larger D becomes. Nonetheless, this single criterion is not adequate to assess the quality of the separation because a few outliers can dominate the RMS of histograms with rare faults. Furthermore, if histograms are systematically non-gaussian, and have tails in different directions this can lead to a large (bad separation) or a negligible overlap (good separation), which is not taken into account by the RMS [11].

3.1.2 The Overlap Criterion

To evaluate the separation of two histograms, for instance normal channels (type 1) and open bonds (type 2), the Overlap Criterion is used. It assesses the fraction OL of incorrectly identified (i. e. as of type 2) channels of type 1, if a threshold is applied at one of the extrema of the histogram of type 2 and vice versa [11]. The value of OL varies from zero overlap to unity if a distribution is completely enclosed by the other one. To evaluate the separation for modules independent of the module geometry in a particular quantity, one considers the fraction of cases where a separation better than $OL < 0.05$ is achieved. This fraction is denoted as $OL_{0.05}$.

3.2 Most Appropriate Tests and Processing

A preselection of appropriately processed test results requires average values of $D > 3$ and $OL < 0.05$ for at least one module geometry in all APV operation modes. From this subset the processed quantities are chosen where D is the largest on average for all geometries and $OL_{0.05}$ is as close as possible to unity. A sufficient set of tests and processing that proved to be well suited for the classification of all kinds of failures independent of the module geometry was identified. These tests are summarised in Table 1.

Test	Processing	Separation of	D	$OL_{0.05}$
Calibration Pulse Amplitude	PERC_0	open bonds short-circuits	$4 \dots 6$ 3.5	$0.33 \dots 1$ 0.93
Gain Slope	PERC_0	open bonds short-circuits	$3 \dots 12$ 3.5	$0.75 \dots 1$ $0.8 \dots 1$
Calibration Pulse Peak Time	CALGR	open bonds	$5 \dots 12$	$OL = 0$ for all geometries (!)
Pinhole Test Amplitude Difference	ABS	pinholes dead channels	32	1
Common Mode Subtracted Noise	ABS	noisy channels	—	—

Table 1: The selected set of quantities and processing methods used for the separation of the respective type of fault, and the corresponding results from the evaluation of the two criteria.

All quantities except for the gain slope data are used for the fault finding algorithm. This algorithm, which is quite involved, is mainly based on the signatures mentioned in sections 2.4 to 2.10. The gain slope data are skipped because initially the gain test was not recommended to be performed in a standard test and a re-analysis of older data should be possible. Nonetheless the stability of the final fault finding algorithm does not suffer from this omission.

4 Assessment of the Fault Finding Efficiency

With the final fault finding algorithm based on the processed test results of Table 1 all previously identified defective channels were found. The classification efficiency of the respective fault type is

- 98% for open bonds between pitch adapter and sensor of one-sensor-modules,
- 88% for open bonds between pitch adapter and sensor of two-sensor-modules,
- 95% for open bonds between the sensors of two-sensor-modules,
- 99% for short-circuited channels,
- 86% for dead channels, and
- 100% for pinholes.

In most cases where the correct identification or the attribution to one of these categories failed, the deviation from normal channel values was not significant. As a result, these channels are marked as "likely" to have a particular type of failure, or as having an "unknown" type of fault. Notably, only 49 normal channels out of about 675,000 were flagged incorrectly.

5 Conclusions

The ARC system and the ARC software provide a setup that is suited to find all known types of defective channels on CMS silicon microstrip modules. In an analysis of data for more than 1,000 data sets for about 500 modules for the tracker endcaps the identification of more than 1,000 defective strips has been optimized by comparing and selecting differently processed quantities out of various correlated qualification tests. The efficiency of detecting the faulty channels is 100% while the rate of classifying correctly the type of fault is higher than 90%. At the same time the rate of mistagged normal channels is only of order 0.01%.

According to the CMS quality criteria for module production only modules of Grade A(B) having less than 1% (2%) flagged channels will be installed in the tracker. Applying these limits to the full production yield of 97.3% this results in 97.6% (2.4%) modules of Grade A(B).

References

[1] The LHC Study Group, *The Large Hadron Collider, Conceptual Design*, CERN/AC/9505, October 1995.

[2] The CMS Collaboration, *Technical Proposal*, CERN/LHCC 94-38 LHCC/P1, 1994.

[3] The CMS Collaboration, *The Tracker Project, Technical Design Report*, CERN/LHCC 98-6, April 1998.

[4] The CMS Collaboration, *Addendum to the CMS Tracker TDR*, CERN/LHCC 2000-016, February 2000.

[5] U. Goerlach, *Front-End Hybrids for the CMS Silicon Tracker*, CERN Report, number 2002-003, page 170. CERN, 2002.

[6] M. J. French, *Design and Results from the APV25, a deep sub micron CMOS front-end chip for the CMS tracker*, NIM A 466, p. 359–365, 2001.

[7] M. Axer et al., *A Test Setup for Quality Assurance of Front-End Hybrids*, CMS Note 2001/046.

[8] M. Axer, *Development of a Test System for the Quality Assurance of Silicon Microstrip Detectors for the Inner Tracking System of the CMS Experiment*. PhD thesis, RWTH Aachen, 2003.

[9] L. Borello, A. Messineo, E. Focardi, A. Macciolo, *Sensor design for the CMS Silicon Strip Tracker*, CMS Note 2003/020.

[10] M. Axer et al., *Test of CMS tracker silicon detector modules with the ARC readout system*, NIM A 518, p. 321–323, 2004.

[11] T. Franke, *Development and Evaluation of a Test System for the Quality Assurance during the Mass Production of Silicon Microstrip Detector Modules for the CMS Experiment*, PhD thesis, RWTH Aachen, 2005.

[12] M. Axer et al., *Tests of Silicon Detector Modules for the Tracker End Cap with the ARC System*, CMS Note 2003/002.